

<sup>5</sup>Sawyer, R. A., "Design and Operation of a Low Speed Gust Tunnel," AGARD CP-174, Wind Tunnel Design and Testing Techniques, London, England, Oct. 1975.

<sup>6</sup>Ham, N. D., Bauer, P. H., and Lawrence, T. L., "Wind Tunnel Generation of Sinusoidal Lateral and Longitudinal Gusts by Circulation Control of Twin Parallel Airfoils," Massachusetts Institute of Technology, Rept. ASRL TR 174-3, Aug. 1974.

<sup>7</sup>Simmons, J. M. and Platzler, M. F., "Experimental Investigation of Incompressible Flow Past Airfoils with Oscillating Jet Flaps," *Journal of Aircraft*, Vol. 8, Aug. 1971, pp. 587-592.

<sup>8</sup>Viets, H., "Flip-Flop Jet Nozzle," *AIAA Journal*, Vol. 13, Oct. 1975, pp. 1375-1379.

<sup>9</sup>Viets, H., Balster, D., and Toms, H. L. Jr., "Time Dependent Fuel Injectors," AIAA Paper 75-1305, AIAA/SAE 11th Propulsion Conference, Anaheim, Calif., 1975.

<sup>10</sup>Viets, H., "High Frequency Gust Tunnel," AGARD Conference Proceedings No. 174 on Windtunnel Design and Testing Techniques, London, England, Oct. 1975.

<sup>11</sup>Piatt, M. and Viets, H., "Conditioned Sampling in an Unsteady Jet," AIAA Paper 79-1857, New York, Aug. 1979.

<sup>12</sup>Viets, H., Ball, M., and Piatt, M., "Experiments in a Subscale Pilot Gust Tunnel," AIAA Paper 80-0453CP, March 1980.

AIAA 81-4144

## Unsteady Gas Dynamic Model of an Arc-Heated Shock Tube

Brian E. Milton\*

*University of New South Wales, Kensington, Australia*  
and

Robert E. Dannenberg†

*NASA Ames Research Center, Moffett Field, Calif.*

### Introduction

**S**MALL volume, conical-shaped arc-drivers utilizing plastic diaphragms that burst concurrently with the start of the arc strike have produced high shock speeds with a simplicity of operation that is attractive.<sup>1,2</sup> Because the optimization of shock-tube performance by experimental means is costly and time consuming, it would be helpful to be able to calculate the actual energy discharged within the arc chamber with the preset driver conditions necessary to achieve a desired shock speed. The gasdynamic performance and the electrical operation of arc-heated shock tubes can be predicted<sup>3</sup> with the use of two newly developed computer codes, EGEN and ERES.<sup>4</sup> EGEN calculates the maximum incident shock Mach number produced in the driven tube as a function of the time history of the energy input to the arc driver and is the subject of this Note.

### EGEN Model and Program

The EGEN model was developed to examine the unsteady gasdynamics of a constant-area, arc-driven shock tube in

which the diaphragm (plastic) bursts immediately with the start of the arc discharge. The arc discharge then continues to heat that proportion of the driver gas which remains in the driver chamber, while the rest of the driver gas expands down the shock tube driving the incident shock wave. The energy addition to the gas during the discharge period referred to in this Note is that transferred by Joule heating only.<sup>5</sup> It is assumed that the process is adiabatic, that the heating is spatially uniform throughout the driver chamber at any one instant, and that the heating is a function of time only. The equation of state of an ideal gas is also assumed. Viscous losses due to shock movement and irreversibilities during wave coalescence have not been considered. Also, as a first-stage solution, the length of the driven tube is not considered. It is merely assumed to be long enough in all cases for the shock reinforcement process to have given the shock its maximum value.

The unsteady gasdynamic calculations were implemented using a stepwise numerical process in which the selected energy input curve, as typified in Fig. 1a, was divided into 40 equal energy increments, the time between increments being determined from the particular curve under examination. Each increment then consisted of an instantaneous energy input followed by a short expansion period when no energy was added. Numerical investigation showed that the solution using 40 increments was within 2% of the asymptotic value when the number of increments approached infinity. There is no restriction on the size or shape of the energy input curve. The EGEN model is therefore well suited to the examination of trends relating to parametric variation of the energy input.

As the energy addition (heating) commenced, the diaphragm burst at time  $t=0$  and a wave pattern formed in the usual way—a shock wave moving downstream and a rarefaction wave moving upstream. Reinforcement of this shock wave then followed due to the driver gas heating. For the chosen increments, instantaneous (i.e., constant-volume) heating allowed a pressure and a temperature rise to be calculated, using the mean driver gas mass. Using this new pressure at the diaphragm station, a matched wave system can be determined by equating the pressure and particle velocities between the two wave systems. Driver outlet pressure, temperature, and gas velocity were thereby determined; they were assumed to remain unchanged for the remaining part of the increment in which no further energy addition took place. During the latter section, constant properties at the driver exit allow the mass flow rate, and hence the total mass efflux during the time period, to be evaluated. The average gas density for the next increment was obtained by subtracting the stepwise decrement and dividing by the known driver chamber volume. The average values for the new state were found by isentropic expansion to this density.

As calculations for each increment were completed, the conditions of the gas at the driver exit were evaluated. The reinforcing process was simplified by expanding this gas isentropically until the pressure and particle velocity matched the increasing values behind the shock. For the shock, as for all EGEN code calculations, the thermodynamic properties were taken from Ref. 6; these have an upper limitation of 5000 K. In the interest of examining the general trends of the model, this temperature was substantially exceeded. Adaptation of the EGEN code, using better high-temperature thermodynamic gas properties of hydrogen, is being undertaken. Also, as an initial simplification, the ideal gas shock-wave equations were used.

The EGEN program was configured primarily to determine the final shock Mach number generated by a specified energy input. The program requires as input data the gas load conditions for the driver and driven tubes, the dimensions of the arc chamber, and the selection of the time rate and magnitude of the energy input. The computations stop if the amount of gas in the driver drops to zero before the 40 increments are completed.

Received Sept. 25, 1980; revision received Jan. 29, 1981. This paper is declared a work of the U. S. Government and therefore is in the public domain.

\*Senior Lecturer, School of Mechanical and Industrial Engineering; also Ames Associate, 1977.

†Research Scientist (Ret.), presently Kendan Associates, Palo Alto, Calif. Associate Fellow AIAA.

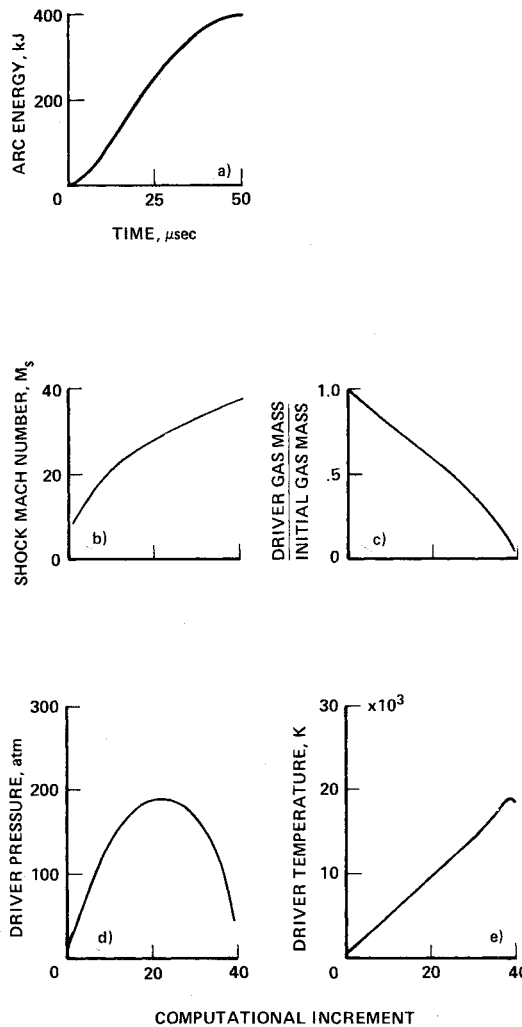


Fig. 1 Typical EGEN program calculations for the 400-kJ, 50- $\mu$ s case.

### Program Calculations and Comparison with Experiment

The energy addition to the driver gas can be computationally controlled in two ways—by a variation in the maximum energy input during a fixed time period or by a variation in the time in which a given maximum energy input occurs. The arc-energy time-history curve shown in Fig. 1a was selected as a base curve representing that developed in achieving the highest experimental shock Mach number,  $M_s = 36$  into 1-Torr hydrogen with the impedance-matched arc driver<sup>7</sup> (IMAD). Curves for different maximum energy input in a given time period or the same energy input over different times were developed as affine transformations of the base curve.

The EGEN computations presented in this paper were arranged primarily to indicate driver requirements to generate the high shock speeds necessary for simulating Jovian entry conditions in a 100-mm-diam shock tube with a 250-mm-long driver. The preset driver and driven tube pressures were 10 atm and 1 Torr hydrogen, respectively. Preset temperatures were 300 K. Figures 1b-1e illustrate the program calculations obtained for the basic energy histogram given in Fig. 1a, a maximum of 400 kJ inputted over a period of 50  $\mu$ s. The results indicated that 1) the shock Mach number continued to increase to its final value during the (heating) computations, 2) the mass of the gas in the chamber decreased, 3) the pressure peaked, and 4) the gas temperature increased. The trends represented in Fig. 1 are typical of those noted for different energy inputs or driver sizes.

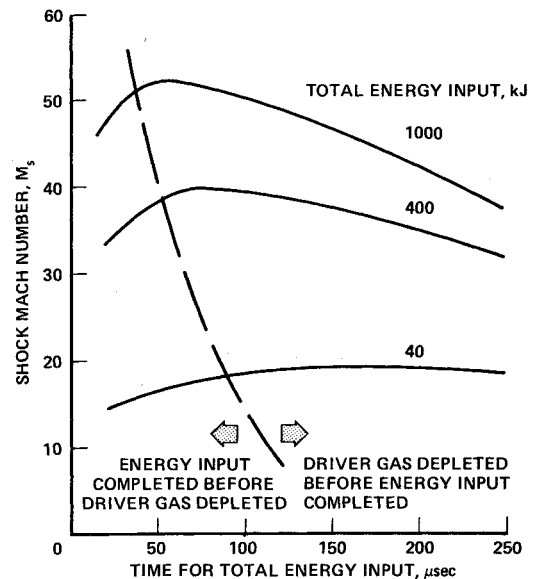


Fig. 2 Shock-speed sensitivity to total time of energy input.

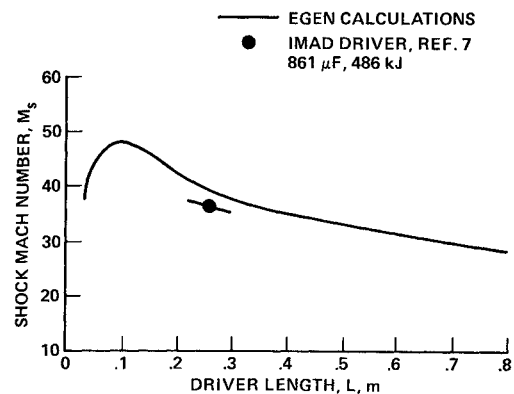


Fig. 3 Shock-speed sensitivity to driver volume.

Figure 2 shows the Mach number variation for the same maximum energy input of 400 kJ as used in the preceding figure with the time period varied parametrically. In addition, results are presented for maximum inputs of 40 and 1000 kJ. In each case, the shock Mach number attained a maximum. Clearly, an optimum time for the energy release is indicated. The time periods for maximum shock Mach number showed close correspondence with those for complete depletion of the driver chamber gas. The latter is indicated by the dashed line in the figure, which denotes the dual conditions that the energy input was completed at the same time that the mass of the driver gas became zero. The adverse effect of insufficient driver gas is quite apparent. At first sight, it might appear that an easy solution to higher performance with a given energy input would be to increase the mass of the gas that is initially in the driver. However, the rate at which the driver pressure rises during the early part of the arc heating is then reduced and overall performance suffers.

Another important result from the calculations was that the selection of driver volume is critical in achieving a high maximum Mach number. This is illustrated in Fig. 3 for the basic 400-kJ, 50- $\mu$ s case. As the length (volume) of the driver was reduced, the shock Mach number increased to a maximum value, after which it declined toward zero as the volume approached zero. The latter would be anticipated, for, obviously, a shock cannot be driven without driver gas. The increase in Mach number as the driver length decreases appears to be due to a higher energy density, which at first offsets the tendency to run out of gas. As the length decreases further, these factors reverse.

The EGEN model shows distinct trends, and it is now apparent that for the production of the highest possible shock speed, the driver arrangement must be tailored to give the proper timing for energy delivery to the driver gas without completely exhausting the gas from the chamber prior to the full deposition of the available energy.

### References

- <sup>1</sup>Menard, W. A., "A Higher Performance Electric-Arc Driven Shock Tube," *AIAA Journal*, Vol. 9, Oct. 1971, pp. 2096-2098.
- <sup>2</sup>Dannenberg, R. E. and Slapnicar, P. I., "Development of Dynamic Discharge Arc Driver with Computer-Aided Circuit Simulation," *AIAA Journal*, Vol. 14, Sept. 1976, pp. 1183-1188.
- <sup>3</sup>Dannenberg, R. E., "GAIM: Gas-Addition, Impedance-Matched Arc Driver," *Proceedings of the 12th International Symposium on Shock Tubes and Waves*, edited by A. Lifshitz and J. Rom, The Magnes Press, Jerusalem, Israel, 1980, pp. 599-606.
- <sup>4</sup>Barnes, G. and Dannenberg, R. E., "Transient Solution for Megajoule Energy Release in a Lumped-Parameter Series RLC Circuit," *Journal of Applied Physics*, Vol. 51, Jan. 1980, pp. 750-753.
- <sup>5</sup>Elkins, R. T. and Baganoff, D., "A Composite Model for a Class of Electric-Discharge Shock Tubes," *Proceedings of the 9th International Symposium on Shock Tubes and Waves*, edited by D. Bershader and W. Griffith, Stanford University Press, Stanford, Calif., 1973, pp. 652-663.
- <sup>6</sup>Van Wylen, G. J., *Thermodynamics*, John Wiley and Son, New York, 1959.
- <sup>7</sup>Dannenberg, R. E., "A New Look at Performance Capabilities of Arc Driven Shock Tubes," *Proceedings of the 11th International Symposium on Shock Tubes and Waves*, edited by B. Ahlborn, A. Hertzberg, and D. Russell, University of Washington Press, Seattle, Wash., 1977, pp. 416-431.

AIAA 81-4145

## Unified Spontaneous Raman and CARS System

S. Lederman\* and C. Posillico†

*Polytechnic Institute of New York, Farmingdale, N. Y.*

### Introduction

HOPE of every experimentalist involved in fluid-dynamics or combustion research has been to find a universal probe capable of simultaneously providing with reasonable accuracy parameters of interest, in a nonintrusive, instantaneous, and remote manner. It appeared for a while that such a probe could be provided by the utilization of the spontaneous Raman scattering techniques. As is well known<sup>1-3</sup> these techniques can provide almost all of the important measurables in a flowfield or flame. Indeed, if a short-time duration high-power laser pulse technique is utilized some of the derived parameters of major importance in turbulent combustion modeling or chemically reacting flows can be obtained easily.

While the preceding is still true for clean flowfields and flames<sup>4-6</sup> in cases where carbon particles or soot is present the appearance of fluorescence, incandescence, and other interfering radiation may make the utilization of the spontaneous Raman scattering techniques very difficult. While certain data acquisition techniques, such as gating, and the utilization of some field polarization properties, etc., may help in improving the signal to noise ratio under difficult conditions, the low scattering cross section of the spontaneous Raman effect has made it necessary to reach into the nonlinear wave mixing phenomena to develop a technique based on the Raman effect that is capable of providing a diagnostic probe several orders of magnitude more efficient in terms of signal strength. This technique, the coherent anti-Stokes Raman scattering technique (CARS) while providing larger signals is not capable of replacing the spontaneous Raman scattering technique in terms of generality. In addition, it generally requires two lasers to provide a single specie or temperature measurement.

In order to provide a more universal diagnostic apparatus, a novel arrangement, based on a simultaneous LDV and spontaneous Raman diagnostic system utilized in Ref. 7, is described here. This arrangement, in its simplest configuration, utilizes a Q-switched ruby laser and a Raman cell filled with a gas of particular interest, whereby stimulation of the Stokes line of the particular gas is caused, and when collinearly mixed with the primary beam generates a CARS signal in a given flowfield. A part of the incident ruby laser is simultaneously utilized to obtain spontaneous Raman signals. Thus, one is able to avail himself of the advantages of both the spontaneous and CARS techniques utilizing only one ruby laser. The system can also be operated using a doubler on the ruby laser. A broadband dye laser, pumped with part of the doubled ruby laser to provide the desired Stokes line when combined with the remainder of the doubled 3471 Å laser line, results in a CARS system. The bulk of the undoubled ruby laser is used to drive a spontaneous Raman system. These systems are described and some preliminary data are shown.

### Theoretical Background

The basic theoretical background of the formulation and operation of both the spontaneous Raman techniques and CARS have been discussed abundantly in the literature. It is therefore sufficient here just to cite some of the references,<sup>1-7</sup> and point out some of the major differences between the spontaneous Raman and the coherent anti-Stokes Raman scattering (CARS) systems.

- 1) Spontaneous Raman is single ended, CARS is not.
- 2) Spontaneous Raman can resolve any number of Raman active species in a mixture simultaneously, CARS can not.
- 3) Spontaneous Raman can provide the temperatures of any number of Raman active species in a mixture simultaneously and simply, CARS can not.
- 4) Spontaneous Raman can provide a measure of the fluctuation of a number of species in a flowfield and thus a measure of turbulent intensity, CARS can not.
- 5) Spontaneous Raman can provide a measure of the mixedness parameters, autocorrelation or correlation of parameters of importance in a flowfield, CARS can not.
- 6) Spontaneous Raman is linear, CARS is not.

These are some of the advantages of spontaneous Raman scattering over CARS.

However, one of the major drawbacks of spontaneous Raman is its extremely low differential scattering cross section. This feature is responsible for very low signal levels and therefore limits the application of spontaneous Raman scattering diagnostics to well-behaved, clean, low noise systems, particularly systems containing essentially no carbon particles or carbon soot. In those cases that are most important in a majority of combustion systems, CARS with its coherent signal, several orders of magnitude higher than the spontaneous Raman signal, is highly preferred in spite of its other limitations.

Received Dec. 2, 1980; revision received Feb. 9, 1981. Copyright © American Institute of Aeronautics and Astronautics, Inc., 1981. All rights reserved.

\*Professor, Aerodynamics Laboratories. Member AIAA.

†Research Assistant, Aerodynamics Laboratories. Student Member AIAA.